International Journal of Innovative Computing, Information and Control
Volume **17**, Number **2**, April **2021**
ICIC International ©2021 ISSN 1349-4198
pp. 639–653

SLIDING MODE FAULT TOLERANT CONTROL OF QUADROTOR UAV WITH STATE CONSTRAINTS UNDER ACTUATOR FAULT

Zixin Wang, Pu Yang, Xukai Hu, Zhiqing Zhang and Chenwan Wen
College of Automation
Nanjing University of Aeronautics and Astronautics
No. 29, Jiangjun Avenue, Jiangning District, Nanjing 211106, P. R. China
ppyang@nuaa.edu.cn

Received October 2020; revised February 2021

Abstract. *Actuator faults and state constraints are the main factors that degrade the performance of quadrotor unmanned aerial vehicle (UAV). In this paper, a robust nonlinear active fault tolerant control algorithm based on nonsingular fast terminal sliding mode control (NFTSMC) and asymmetric barrier Lyapunov function is designed for a quadrotor UAV system with actuator fault and unknown external disturbance while specifically considering state constraints. Firstly, since the uncertainty of fault magnitudes, an adaptive estimator is applied to estimating the severity of actuator faults. Then, a novel NFTSMC is proposed. In virtue of the proposed method, the system can not only own strong robustness but also reach the original value in a short finite-time. In addition, aiming at the phenomenon of state constraints in the actual flight of quadrotor aircraft, the asymmetric barrier Lyapunov function (BLF) is introduced to guarantee the constraints not to be violated. Finally, the effectiveness and superiority of the proposed control scheme are verified by contrast simulation and comparison experiments.*
Keywords: Quadrotor UAV, Fault tolerant control, State constraints, Sliding mode control, Barrier Lyapunov function

1. **Introduction.** In recent years, unmanned aerial vehicles (UAVs) have attracted tremendous attention from both military and civil fields. Quadrotor is one of the most popular kinds of rotating wings UAVs. Compared with other kinds of UAVs, quadrotor has many advantages such as vertical take-off and landing, hovering, low cost, lightweight, high agility and maneuverability [1]. Based on these properties, quadrotor is employed in various environments to accomplish complex missions, such as fire fighting, surveillance, mapping and aerial photography [2,3]. However, some special applications and environments may threaten the safety and stability of quadrotor [4]. Even in a component level, any failure may influence the whole system and damage the quadrotor itself [5]. Therefore, the design of fault-tolerant control (FTC) scheme which can deal with faults and disturbances is vital and has significant research value.

In essence, the fault is that the system's parameters or eigenvalues deviate from the standard value. Over the last decades, lots of classical fault-tolerant control strategies have been proposed for the flight control problem of quadrotor helicopters [6-8]. In general, the FTC methods can be classified into two types, known as active FTC (AFTC) and passive FTC (PFTC). Early research of fault-tolerant is about PFTC, which is essentially an extension of robust control. The PFTC methods are designed to be robust to deal with presumed faults without online detection of faults [9], such as sliding mode control and quantitative feedback theory [10-13]. In [14] an SMC is presented to cope with actuator effectiveness fault of a class of uncertainty systems with time delay. Considering the

DOI: 10.24507/ijicic.17.02.639

change of structural parameters caused by failure, an adaptive sliding mode controller was designed in [15] to increase the robustness of satellite attitude system. PFTC has no diagnosis module and no additional hardware, so it has the advantages of low cost, simple design process and easy implementation. However, it has limited fault-tolerance capability and may sacrifice nominal performance [16].

In contrast with PFTC, AFTC is based on reconfiguring the controllers with the help of fault detection and diagnosis (FDD) scheme that provides the fault data online [17,18]. In terms of a nonlinear multiple-input multiple-output (MIMO) system, an adaptive actuator failure compensation scheme is given in [19] including multiple estimators and controllers. In [20], a parallel bank of recurrent neural networks is designed to precisely estimate the faults of quadrotor helicopter. In order to address external disturbance and actuator faults of a UAV, [21] proposed a fixed-time observer-based fixed-time fault-tolerant controller using the integral-type SMC.

In practice, state constraints are inevitable for quadrotor during many practical flight missions. For example, when transporting goods, large attitude angle changes may lead to sloshing. The ignorance of constraints may degrade the control performance or even lead to a catastrophic crash. Thus, the state constraint consideration is crucial for quadrotor control system design. In recent years, some achievements about state constraints have been proposed, such as mode predict control [22], reference governors [23], and constraint-handling methods based on set invariance [24]. Moreover, [25] proposed barrier Lyapunov function (BLF) which grows to infinite when its arguments approach the limit, so that the constraints are guaranteed to be obeyed. In [26], a BLF-based backstepping controller is proposed for single-input single-output (SISO) nonlinear systems to prevent constraint violation. On this basis, [21] designed a control scheme based on asymmetric time-varying BLF and backstepping control for a multi-rotor UAV with time-varying output constraints. The combination of BLF and backstepping control is common, but the backstepping-based control schemes will suffer from the explosion of complexity for high-order nonlinear systems.

Inspired by the challenges mentioned above, this study investigates the fault-tolerant control problem of quadrotor in the presence of state constraints. A novel SMC associated with BLF is developed to guarantee the stability of UAV with state constraints and prevent the main drawback of explosion of complexity. The main contributions of this paper are as follows.

1) An active FTC approach is addressed to deal with actuator faults and external disturbance. The fault information can be obtained by applying the proposed observer.

2) A novel nonsingular fast terminal sliding mode based control law is developed to come true high precision tracking performance and fixed-time convergence.

3) Barrier Lyapunov function is introduced to keep the sliding mode surface within a certain range to ensure the constraints not to be transgressed.

The remainder of this paper is organized as follows. The dynamic mode of the quadrotor is briefly described in Section 2. Section 3 proposed an estimator and the nonsingular fast terminal sliding mode controller in conjunction with BLF. The relative experiments are followed in Section 4 to show the excellent performance of this method. Finally, the conclusions of this work are presented in Section 5.

2. **Preliminaries and Problem Formulation.**

2.1. **The model description.** The plant considered in this paper is quadrotor UAV, whose model is shown in Figure 1. The quadrotor UAV is a strongly coupled and underdriven system with four motors and propellers as inputs to provide thrust force for it.

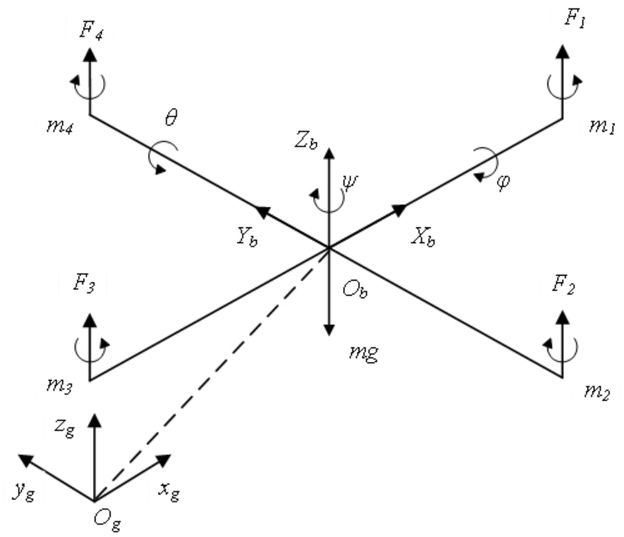

Figure 1. Model of quadrotor UAV

The propellers are driven through the rotation of the brushless DC motors. The attitude and position of the aircraft can be controlled by adjusting the speed of the motor.

As shown in the figure, the motors are represented as m_i ($i = 1, 2, 3, 4$) and forces generated by them are F_i ($i = 1, 2, 3, 4$). $\Theta = [\phi, \theta, \psi]^T$ represents the Euler angle (roll, pitch, yaw), m and g represent the mass of UAV and gravity respectively. The adjacent propellers rotate in opposite directions, and such rotation in opposite directions can offset the counter-torque generated by the propeller (motor) rotation, so as to ensure a stable forward direction of the aircraft. The yaw movement is obtained by a rotation difference between two adjacent propellers and the rotation difference between two opposite propellers generates pitch and roll movement.

2.2. **Quadrotor kinematics.** To describe the quadrotor attitude dynamics, two coordinate systems need to be considered. As shown in Figure 1, the inertia frame $E_g = \{O_g x_g y_g z_g\}$ is fixed with respect to the ground and the body-fixed frame $E_b = \{O_b x_b y_b z_b\}$ is located at the center mass of quadrotor. $P = [x, y, z]^T$ represents the absolute position (inertia frame); $\Omega = [p, q, r]^T$ and $V = [u, v, w]^T$ represent Euler's angular velocity and the linear velocity of the body in the ground coordinate system. Translation matrix describes the angular velocity relationship between the body and the inertial frame. The matrix R describes the transformation relationship between the two coordinate systems.

The rotation matrix from the inertial frame to the body frame is denoted as R_E^B. The rotation matrix from the body frame to the inertial frame is, R_B^E then [27]:

$$R_B^E = \left(R_E^B\right)^{-1} = \begin{bmatrix} \cos\theta\cos\psi & \cos\psi\sin\theta\sin\psi - \sin\psi\cos\phi & \cos\psi\sin\theta\cos\phi + \sin\psi\sin\phi \\ \cos\theta\sin\psi & \sin\psi\sin\theta\sin\phi + \cos\psi\cos\phi & \sin\psi\sin\theta\cos\phi - \cos\psi\sin\phi \\ -\sin\theta & \sin\phi\cos\theta & \cos\phi\cos\theta \end{bmatrix} \tag{1}$$

Define U_ϕ, U_θ, U_ψ, U_z as the control input of the four independent control channels of the quadrotor, and the control input of the system is

$$\begin{cases} U_\phi = l(F_3 - F_4) \\ U_\theta = l(F_1 - F_2) \\ U_\psi = \tau_1 + \tau_2 - \tau_3 - \tau_4 \\ U_z = F_1 + F_2 + F_3 + F_4 \end{cases} \tag{2}$$

where l is the distance between the centre mass of the aircraft and the centre of the propeller, F_i $(i = 1, 2, 3, 4)$ is the force produced by the propeller and τ_i $(i = 1, 2, 3, 4)$ is the counter-torque produced by the propeller.

The relationship between the force F_i, the counter-torque τ_i and the motor speed ω_i is

$$\begin{cases} F_i = b{\omega_i}^2 \\ \tau_i = d{\omega_i}^2 \end{cases} \tag{3}$$

where b and d are corresponding coefficients. According to Newton's second law [28]:

$$\begin{aligned} \ddot{P} = \begin{bmatrix} \dot{u} \\ \dot{v} \\ \dot{w} \end{bmatrix} &= \frac{1}{m}\left(R_B^E \begin{bmatrix} 0 \\ 0 \\ U_z \end{bmatrix} - \begin{bmatrix} 0 \\ 0 \\ mg \end{bmatrix} \right) \\ &= \frac{1}{m} \begin{bmatrix} (\cos\psi\sin\theta\cos\phi + \sin\psi\sin\phi)U_z \\ (\sin\psi\sin\theta\cos\phi - \cos\psi\sin\phi)U_z \\ (\cos\phi\cos\theta)U_z - mg \end{bmatrix} \end{aligned} \tag{4}$$

According to Newton-euler formula, the resultant moment can be expressed in two forms:

$$\sum M^b = J_b\dot{\Theta} + \Theta \times J_b\Omega = U_R - K \tag{5}$$

where $U_R = [U_\phi, U_\theta, U_\psi]^T$, J_b is the inertia matrix in body frame, $J_b = diag\{J_x, J_y, J_z\}$, and K is air friction, $K = \left[k_\phi p^2, k_\theta q^2, k_\psi r^2\right]^T$, where k_ϕ, k_θ, k_ψ are drag coefficients. Calculating the two expressions in Equation (5) separately, we can obtain that

$$\begin{aligned} J_b\dot{\Theta} + \Theta \times J_b\Omega &= \begin{bmatrix} J_x & 0 & 0 \\ 0 & J_y & 0 \\ 0 & 0 & J_z \end{bmatrix} \begin{bmatrix} \dot{p} \\ \dot{q} \\ \dot{r} \end{bmatrix} + \begin{bmatrix} p \\ q \\ r \end{bmatrix} \times \begin{bmatrix} J_x & 0 & 0 \\ 0 & J_y & 0 \\ 0 & 0 & J_z \end{bmatrix} \begin{bmatrix} p \\ q \\ r \end{bmatrix} \\ &= \begin{bmatrix} J_x\dot{p} \\ J_y\dot{q} \\ J_z\dot{r} \end{bmatrix} + \begin{bmatrix} qr(J_z - J_y) \\ rp(J_x - J_z) \\ qp(J_y - J_x) \end{bmatrix} = \sum M^b \end{aligned} \tag{6}$$

$$U_R - K = \begin{bmatrix} U_\phi - k_\phi p^2 \\ U_\phi - k_\theta q^2 \\ U_\phi - k_\psi r^2 \end{bmatrix} = \sum M^b \tag{7}$$

Combining Equations (4), (6) and (7), we can obtain that

$$\begin{cases} \dot{u} = \dfrac{1}{m}(\cos\phi\sin\theta\cos\psi + \sin\phi\sin\psi)U_z \\ \dot{v} = \dfrac{1}{m}(\cos\phi\sin\theta\sin\psi - \sin\phi\cos\psi)U_z \\ \dot{w} = \dfrac{1}{m}(\cos\phi\cos\theta)U_z - g \\ \dot{p} = \dfrac{1}{J_x}\left(qr(J_y - J_z) + U_\phi - k_\phi p^2\right) \\ \dot{q} = \dfrac{1}{J_y}\left(rp(J_z - J_x) + U_\theta - k_\theta q^2\right) \\ \dot{r} = \dfrac{1}{J_z}\left(pq(J_x - J_y) + U_\psi - k_\psi r^2\right) \end{cases} \tag{8}$$

2.3. **Problem formulation.** The dynamic model is described by state space expression, and Equation (8) can be rewritten into the following form:

$$\begin{cases} \dot{x}_{i1} = x_{i2} \\ \dot{x}_{i2} = f_i(x) + b_i(1-\sigma_i)U_i + d_i \qquad (i = 1, 2, 3, 4, 5, 6) \\ y_i = x_{i1} \end{cases} \tag{9}$$

where $x_{i1} = (x, y, z, \phi, \theta, \psi)^T$, $x_{i2} = (u, v, w, p, q, r)^T$, f_i and b_i are determined by Equation (8), d_i is external disturbance and U_i is virtual control quantity:

$$\begin{cases} U_1 = (\cos\phi\sin\theta\cos\psi + \sin\phi\sin\psi)U_z \\ U_2 = (\cos\phi\sin\theta\sin\psi - \sin\phi\cos\psi)U_z \\ U_3 = (\cos\phi\cos\theta)U_z \\ U_4 = U_\phi \\ U_5 = U_\theta \\ U_6 = U_\psi \end{cases} \tag{10}$$

$0 \leq \sigma_i \leq 1$ shows the failure rate of ith control chunnel. State $x_{i1}(t)$ needs to satisfy following constraints:

$$\underline{k}_{ci} < x_{i1}(t) < \overline{k}_{ci}, \quad \forall t \geq t_0 \tag{11}$$

where $\underline{k}_{ci} < \overline{k}_{ci}$, $\underline{k}_{ci}$ and $\overline{k}_{ci}$ are constants.

This paper aims to design an appropriate estimator and sliding mode controller against actuator faults and external disturbance, so that the desired trajectories can track the task of UAV system with strong robustness, simultaneously, the output states within the constraints sets during operation. In order to achieve the target, the following assumptions and lemmas are used in this paper [29].

Assumption 2.1. *Function $b_i(x_i)$, $i = 1, 2, \ldots, 6$ are known and there is a positive constant, b_0 satisfying $0 < b_0 \leq |b_i(x_i)|$ for any $\underline{k}_{ci} < y_i(t) < \overline{k}_{ci}$. Without loss of generality, suppose that all $b_i(x_i)$ are positive.*

Assumption 2.2. *There are constants $\underline{Y}_{i0}, \overline{Y}_{i0}, Y_{i1}, \ldots, Y_{in}$, satisfying $\underline{k}_{ci1} < \underline{Y}_{i0} < \overline{Y}_{i0} < \overline{k}_{ci1}$, and for the expected output $y_{id}(t)$ and their derivative satisfying $\underline{Y}_{i0} \leq y_{id}(t) \leq \overline{Y}_{i0}, |\dot{y}_{id}| < Y_{i1}, |\ddot{y}_{id}| < Y_{i2}, \ldots, \left|y_{id}^{(n)}\right| < Y_n$, $\forall t \geq t_0$ $(i = 1, 2, \ldots, 6)$.*

Assumption 2.3. *The external disturbance d_i is usually unknown and assumed to be bounded and its upper limit is known: $|d_i| \leq \delta$, where δ is a positive constant.*

Lemma 2.1. *For any positive constants k_l, k_r, let $Z = \{z \in R : -k_l < z < k_r\} \subset R$ and $N := R^l \times Z \subset R^{l+1}$ be open sets. The following system can be concerned:*

$$\dot{\eta} = h(t, \eta) \tag{12}$$

where $\eta := [w, z]^T \in N, h : R_+ \times N \to R^{l+1}$ is piecewise continuous in t and locally Lipschitz. Suppose that there exist functions $P := Z \to R^+$ and $Q := R^l \to R^+$ continuously differentiable and positive definite in their respective domains, such that

$$\gamma_1(\|w\|) \leq P(w) \leq \gamma_2(\|w\|) \tag{13}$$

$$Q(z) \to \infty \ \textit{as} \ z \to -k_l \ \textit{or} \ z \to k_r \tag{14}$$

where γ_1, γ_2 are K_∞ class functions, let $V(\eta) = P(w) + Q(z)$, $z(0) \in Z$, if the inequality holds:

$$\dot{V} = \frac{\partial V}{\partial \eta} h \leq 0 \tag{15}$$

then $z \in Z$, $\forall t \in [t_0, \infty)$.

Lemma 2.2. *For any* $|\xi| < 1$, *the inequality* $\ln \frac{1}{1-\xi^2} < \frac{\xi^2}{1-\xi^2}$ *holds.*

3. **Fault-tolerant Control Laws Design.** In this section, an active FTC is presented to simultaneously deal with actuator faults and output constraints for a UAV. We first design an adaptive estimator to estimate the failure values for all failure patterns. Then an NFTSMC is designed against disturbances and model uncertainties to achieve null steady-state error tracking in a short finite-time. Subsequently, an asymmetric barrier Lyapunov function is developed to guarantee that the output constraints are not violated at any time, including the transient phase adaptation.

3.1. **Estimator design.** The mathematical model is manipulated into a state space form:

$$\begin{cases} \dot{X}(t) = AX(t) + BU + F(x) + Dd - BEU \\ Y(t) = CX(t) \end{cases} \tag{16}$$

where $X(t)$ represents the state variables, $Y(t)$ is the output vector, U is the control input vector and B is the control effectiveness matrix. $E = diag\{\sigma_1, \sigma_2, \ldots, \sigma_6\}$ represents the failure rate of actuator. The estimator is obtained by using some assumptions as follows.

Assumption 3.1. (A, C) *is observable,* $\exists K$ *denote* $A_1 = A - KC$, *which satisfies that all eigenvalues of* A_1 *have negative real parts.*

Assumption 3.2. *There exist a positive Lipschitz constant* γ, *such that* $\|F(x_1) - F(x_2)\| \leq \gamma \|x_1 - x_2\|$.

Assumption 3.3. *For any positive definite symmetric matrix* Q, *there exists a unique positive definite symmetric matrix* P *satisfying* $A_1^T P + PA_1 = -Q$.

Assumption 3.4. *There exists a matrix* R *satisfying* $PD = (RC)^T$.

According to Equation (16) the corresponding estimator is designed as

$$\begin{cases} \dot{\hat{X}}(t) = A\hat{X}(t) + BU + F(\hat{x}) + Dv - B\hat{E}U + K\left[\hat{Y}(t) - Y(t)\right] \\ \hat{Y}(t) = C\hat{X}(t) \end{cases} \tag{17}$$

where $\hat{X}(t)$, $\hat{E}$ and $\hat{Y}(t)$ denote the estimated values of $X(t)$, E and $Y(t)$ respectively.

$$v = \begin{cases} -\delta \dfrac{R\tilde{Y}(t)}{\left\|R\tilde{Y}(t)\right\|}, & \tilde{Y}(t) \neq 0 \\ 0, & \tilde{Y}(t) = 0 \end{cases} \tag{18}$$

The parameter matrix is amended by the adaptive law:

$$\dot{\hat{E}} = -\Gamma L\tilde{Y}(t)U^T \tag{19}$$

where Γ is a positive definite symmetric matrix, $\tilde{Y}(t) = \hat{Y}(t) - Y(t)$, L satisfies $PB = C^T L^T$. According to [30], $\lim_{t\to\infty} \hat{E} - E = 0$.

3.2. **Fault tolerant controller design.** The error tracking is designed as

$$\begin{cases} e_{i1} = y_i - y_{id} = x_{i1} - y_{id} \\ e_{i2} = \dot{e}_{i1} = x_{i2} - \dot{y}_{id} \end{cases} \tag{20}$$

Denote the sliding surface for the system can be designed as

$$S_i = e_{i1} + k_{i1}|e_{i1}|^{\alpha_i} sign(e_{i1}) + k_{i2}|e_{i2}|^{\beta_i} sign(e_{i2}) \tag{21}$$

where k_{i1} and k_{i2} are positive constants, $1 < \beta_i < 2$ and $\beta_i < \alpha_i$. The time derivative of sliding surface can be given as

$$\dot{S}_i = e_{i2} + \alpha_i k_{i1}|e_{i1}|^{\alpha_i-1} e_{i2} + \beta_i k_{i2}|e_{i2}|^{\beta_i-1} \dot{e}_{i2} \tag{22}$$

In order to meet the control requirements, the control law is given as

$$\begin{aligned} U_i &= U_{eq} + U_{sw} \\ U_{eq} &= \frac{1}{b_i(1-\sigma_i)}\left[-f_i(x) + \ddot{y}_d - \frac{|e_{i2}|^{2-\beta_i}}{\beta_i k_{i2}}\left(1 + \alpha_i k_{i1}|e_{i1}|^{\alpha_i-1}\right) sign(e_{i2})\right] \\ U_{sw} &= \frac{1}{b_i(1-\sigma_i)}\left[-p_i S_i - \delta sign(S_i)\right] \end{aligned} \tag{23}$$

where $p_i > 0$ is the switching gain and δ is upper limit of the disturbance.

Lemma 3.1. *When the initial error $e_{i1}(t_0)$ satisfies*

$$k_{ai} < e_{i1}(t_0) < k_{bi} \tag{24}$$

and the system is stable, the inequality $\underline{k}_{ci} < x_{i1}(t) < \overline{k}_{ci}$, $\forall t \geq t_0$ holds if

$$k_{ai} < S_i < k_{bi} \tag{25}$$

$$\begin{cases} k_{ai} = \underline{k}_{ci} - \underline{Y}_{i0} \\ k_{bi} = \overline{k}_{ci} - \overline{Y}_{i0} \end{cases} \tag{26}$$

Proof: First, Equation (21) can be written as

$$S_i = \left(1 + k_{i1}|e_{i1}|^{\alpha_i-1}\right) e_{i1} + k_{i2}|e_{i2}|^{\beta_i-1} e_{i2} = h_{i1} e_{i1} + h_{i2} \dot{e}_{i1} \tag{27}$$

where h_{i1}, h_{i2} are constants $h_{i1} \geq 1$, $h_{i2} \geq 0$. According to Assumption 3.3 and Equation (20), we know that $e_{i1}(t)$ is continuous differentiable, which means $\dot{e}_{i1} = 0$ or $t = t_0$ or $t \to \infty$ as $e_{i1}(t) = e_{i1\max}$ or $e_{i1}(t) = e_{i1\min}$.

Considering the system is stable, we obtain $e_{i1}(t) \to 0$ as $t \to \infty$, so that

$$k_{ai} < e_{i1}(\infty) < k_{bi} \tag{28}$$

Suppose that $e_{i2} = \dot{e}_{i1}(t)$ has m zeros, when $t = t_i$, $i = 1, 2, \ldots, m$, $\dot{e}_{i1}(t_i) = 0$, Equation (27) can be written as

$$S_i = h_{i1} e_{i1}(t_i) \tag{29}$$

According to Equation (26) and Assumption 2.2, we know that $k_{ai} < 0 < k_{bi}$. Then from Equations (25) and (29), we conclude that

$$k_{ai} < \frac{k_{ai}}{h_{i1}} < e_{i1}(t_i) < \frac{k_{bi}}{h_{i1}} < k_{bi} \tag{30}$$

Combining (24), (29) and (30), we obtain $k_{ai} < e_{i1}(t) < k_{bi}$ for any $t > t_0$, which is equal to $\underline{k}_{ci} < x_{i1}(t) < \overline{k}_{ci}$, $\forall t \geq t_0$.

Theorem 3.1. *Consider the closed loop system (9) with asymmetric constraints (11). Under Assumptions 2.1, 2.2 and 2.3, control law designed as (23), if the initial state satisfies $\underline{k}_{ci} < x_{i1}(0) < \overline{k}_{ci}$, then the following properties hold.*

1) The asymmetric state constraints are never transgressed.

2) The system states converge to the sliding surface in a finite time.

Proof: Consider the following barrier Lyapunov function:

$$V = \frac{q(S_i)}{2}\ln\frac{k_{bi}^2}{k_{bi}^2 - {S_i}^2} + \frac{1-q(S_i)}{2}\ln\frac{k_{ai}^2}{k_{ai}^2 - {S_i}^2} \tag{31}$$

where $q(S_i) = 1$ when $S_i > 0$ and $q(S_i) = 0$ when $S_i \leq 0$. For simplicity, we abbreviate $q(S_i)$ by q, throughout this paper. The time derivative of V is

$$\dot{V} = \left(\frac{q}{k_{bi}^2 - {S_i}^2} + \frac{1-q}{k_{ai}^2 - {S_i}^2}\right) S\dot{S} \tag{32}$$

By substituting Equations (20)-(22) into Equation (31), the dynamic of V can be written as

$$\dot{V} = \left(\frac{q}{k_{bi}^2 - {S_i}^2} + \frac{1-q}{k_{ai}^2 - {S_i}^2}\right) \beta_i k_{i2} |e_{i2}|^{\beta_i - 1}\left[d_i S_i - p{S_i}^2 - \delta\,|S_i|\right] \tag{33}$$

According to Assumption 2.3, it is easy to verify that

$$\begin{aligned}\dot{V} &\leq \left(\frac{q}{k_{bi}^2 - {S_i}^2} + \frac{1-q}{k_{ai}^2 - {S_i}^2}\right) \beta_i k_{i2} |e_{i2}|^{\beta_i - 1}\left[-p{S_i}^2 - (d_i - \delta)\,|S_i|\right] \\ &\leq -p\beta_i k_{i2}|e_{i2}|^{\beta_i-1}\left(\frac{q}{k_{bi}^2 - {S_i}^2} + \frac{1-q}{k_{ai}^2 - {S_i}^2}\right){S_i}^2 \leq 0\end{aligned} \tag{34}$$

1) According to the definitions of k_{ai} and k_{bi} in Equation (26), the initial condition requirement is set as $\underline{k}_{ci} < x_{i1}(t_0) < \overline{k}_{ci}$. This is equal to $k_{ai} < S_i(t_0) < k_{bi}$, then Lemma 2.1 ensures that $k_{ai} < S_i(t) < k_{bi}$, $\forall t \geq t_0$. Since Lemma 3.1, we can conclude that $\underline{k}_{ci} < x_{i1}(t) < \overline{k}_{ci}$, $\forall t \geq t_0$.

2) According to Lemma 2.2 and Equation (34), we can infer that

$$\begin{aligned}\dot{V} &\leq -p\beta_i k_{i2}|e_{i2}|^{\beta_i-1}\left(\frac{q}{k_{bi}^2 - {S_i}^2} + \frac{1-q}{k_{ai}^2 - {S_i}^2}\right){S_i}^2 \\ &\leq -2p\beta_i k_{i2}|e_{i2}|^{\beta_i-1}\left(\frac{q}{2}\ln\frac{k_{bi}^2}{k_{bi}^2 - {S_i}^2} + \frac{1-q}{2}\ln\frac{k_{ai}^2}{k_{ai}^2 - {S_i}^2}\right) \\ &= -2p\beta_i k_{i2}|e_{i2}|^{\beta_i-1}V\end{aligned} \tag{35}$$

By defining $h = 2p\beta_i k_{i2}|e_{i2}|^{\beta_i-1}$, Equation (35) can be written as

$$\frac{dV}{dt} \leq -hV \tag{36}$$

After some simple calculation, we can obtain that

$$dt \leq -\frac{dV}{hV} \tag{37}$$

Suppose that the reaching time from the initial state error $e_{i1}(t_0) \neq 0$ to $e_{i1}(t) = 0$ is t_r. Now, taking integral of both sides of Equation (36) from $e_{i1}(t_0)$ to $e_{i1}(t_r)$, one can obtain

$$t_r \leq t_0 + \frac{1}{h}\ln V \tag{38}$$

This completes the proof above.

4. **Simulation.** In this scenario, numerical simulations are performed to validate the performance of the proposed NFTSMC based fault-tolerant flight controller in conjunction with ABLF. In order to show the superiority of the proposed approach, contrast experiments with two other traditional controllers are implemented. One is a sliding mode based active fault-tolerant controller similar to [31], marked as method 1, and the other is backstepping algorithm based on BLF marked as method 2. The algorithm proposed in this paper is marked as method 3.

The main physical parameters of the quadrotor are shown as follows. The inertia matrix of UAV is $J = diag\{0.04, 0.04, 0.08\}$ (kg·m^2), the mass is $m = 1.7$ kg and the air drag coefficients are $k_\varphi = k_\theta = k_\phi = 6 \times 10^{-3}$. Without loss of generality, the initial Euler angle is set as $\Theta(0) = [-0.2, -0.2, 0.5]^T$ (rad) and the initial angular velocity is chosen as $\dot{\Omega}(0) = [0, 0, 0]^T$ (rad/s). The initial position and speed are $P(0) = [0, 1, 0.3]^T$ (m), $V(0) = [0, 0, 0]^T$ (m/s).

Remark 4.1. *According to Equation (8), the changes of physical parameters can only influence the values of f_i and b_i, so the results of this simulation can represent the effects of this method with different settings.*

4.1. **Simulation 1.** Considering the uncertainty of external disturbance, we set white noise with upper bound $\delta = 0.5$ as the disturbance. And the the fault model is

$$\sigma_2 = \begin{cases} 0.3, & t \in [6, 12] \\ 0, & t \in [0, 6) \cup (12, 20] \end{cases} \tag{39}$$
$$\sigma_5 = \begin{cases} 0.4, & t \in [4, 14] \\ 0, & t \in [0, 4) \cup (14, 20] \end{cases}$$
$$\sigma_1 = \sigma_3 = \sigma_4 = \sigma_6 = 0$$

The fault information obtained form estimators proposed in method 1 and method 3 is illustrated in Figure 2 and Figure 3 separately. Figure 2 and Figure 3 show that both methods can get correct fault information when dealing with actuator failures. The proposed estimator can detect the faults in about 0.5 seconds, and the estimator in method 1 needs about 1.5 seconds. By comparing Figure 2 and Figure 3, we can conclude that method 3 converges more rapidly and steadily than method 1.

4.2. **Simulation 2.** For FTC described in 3.2, the parameters of the controller are chosen as $\alpha_i = 2$, $\beta_i = 1.67$, $k_{i1} = 1$, $k_{i2} = 1$, $p = 5$. Consider the actual flight characteristics of UAV, the desired trajectory of the attitude and the position are set as

$$[y_{4d}, y_{5d}, y_{6d}]^T = [0.4\sin(t), 0.3\cos(t), 0.3]^T \text{ (rad)} \tag{40}$$
$$[y_{1d}, y_{2d}, y_{3d}]^T = [0.5, 0.5, 0.8]^T \text{ (m)} \tag{41}$$

And the constraints are set as

$$\left[\overline{k}_{c4}, \underline{k}_{c4}, \overline{k}_{c5}, \underline{k}_{c5}, \overline{k}_{c6}, \underline{k}_{c6}\right]^T = [0.6, -0.6, 0.5, -0.5, 0.7, 0.2]^T \text{ (rad)} \tag{42}$$
$$\left[\overline{k}_{c1}, \underline{k}_{c1}, \overline{k}_{c2}, \underline{k}_{c2}, \overline{k}_{c3}, \underline{k}_{c3}\right]^T = [0.9, -0.2, 1.3, 0.1, 1.2, 0]^T \text{ (m)} \tag{43}$$

The disturbance has up bound $\delta = 0.5$ and 30% failure acts on the fourth channel after 5 s. The simulation results of method 1, 2, 3 are shown in Figures 4-9. Figures 4-6 are tracking results of attitude channels, and Figures 7-9 are tracking results of position channels.

From Figures 4-9, it can be seen that in the beginning, each method can finally track the desired trajectory after a few seconds of adjustment. The curves fluctuated after 5 seconds, which means that the faults have occurred.

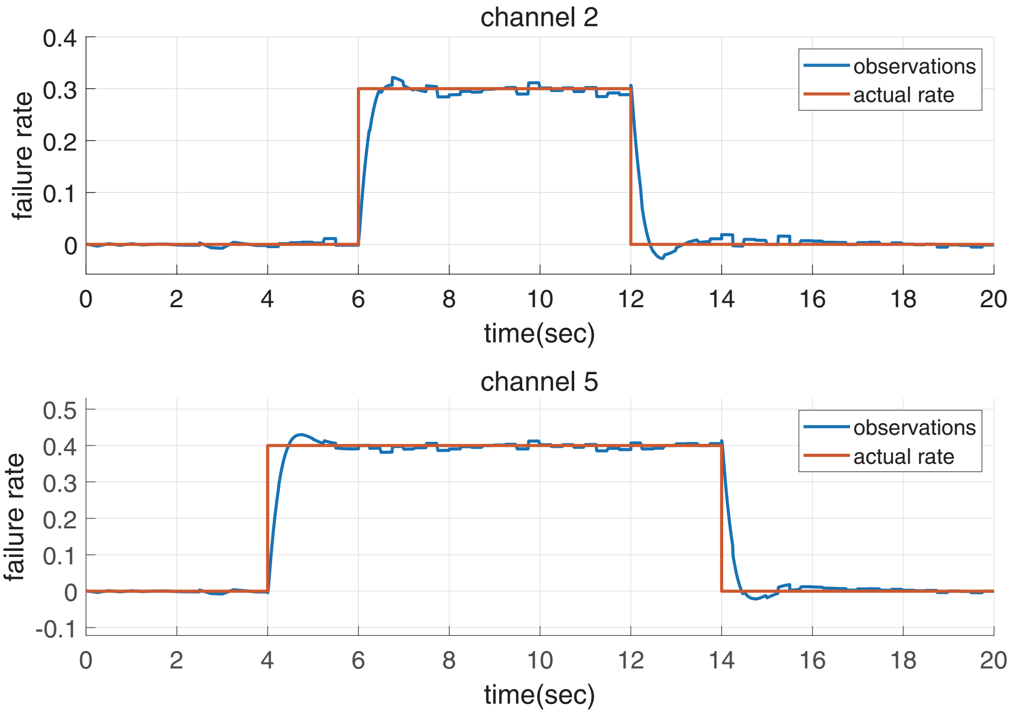

FIGURE 2. FDD results of method 1

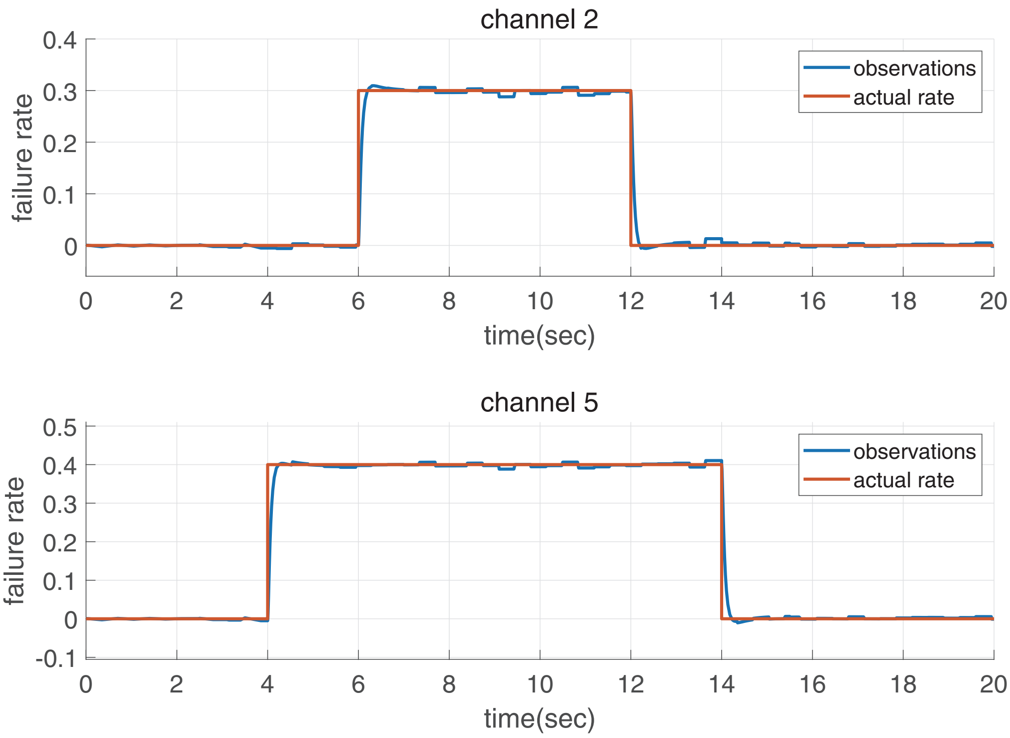

FIGURE 3. FDD results of method 3

By comparing 3 curves in Figures 4-9, we can see that method 1 and method 3 can converge again. Compared with method 3, the adjust time of method 1 is very long, and the overshoot is too large to meet the constraints for all channels without BLF. As for traditional backstepping method based on BLF (method 2), the overshoot is much smaller

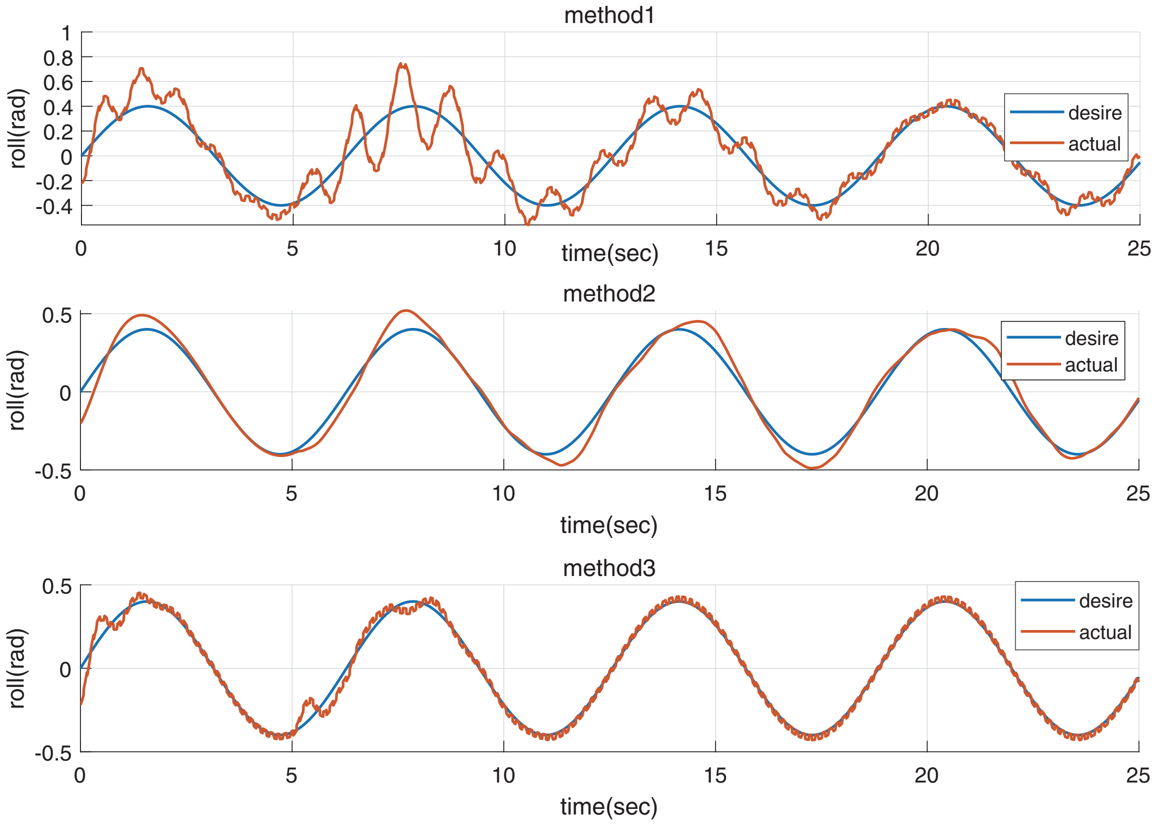

Figure 4. Time response of roll

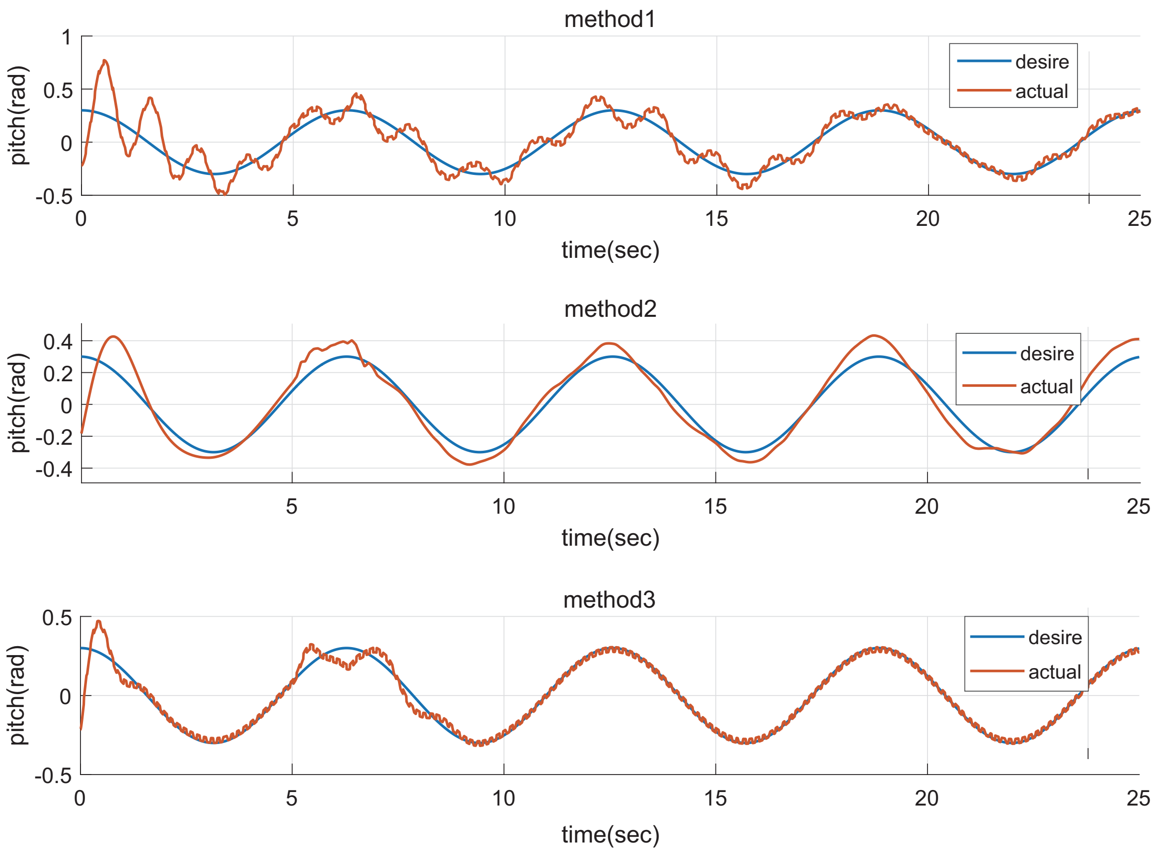

Figure 5. Time response of pitch

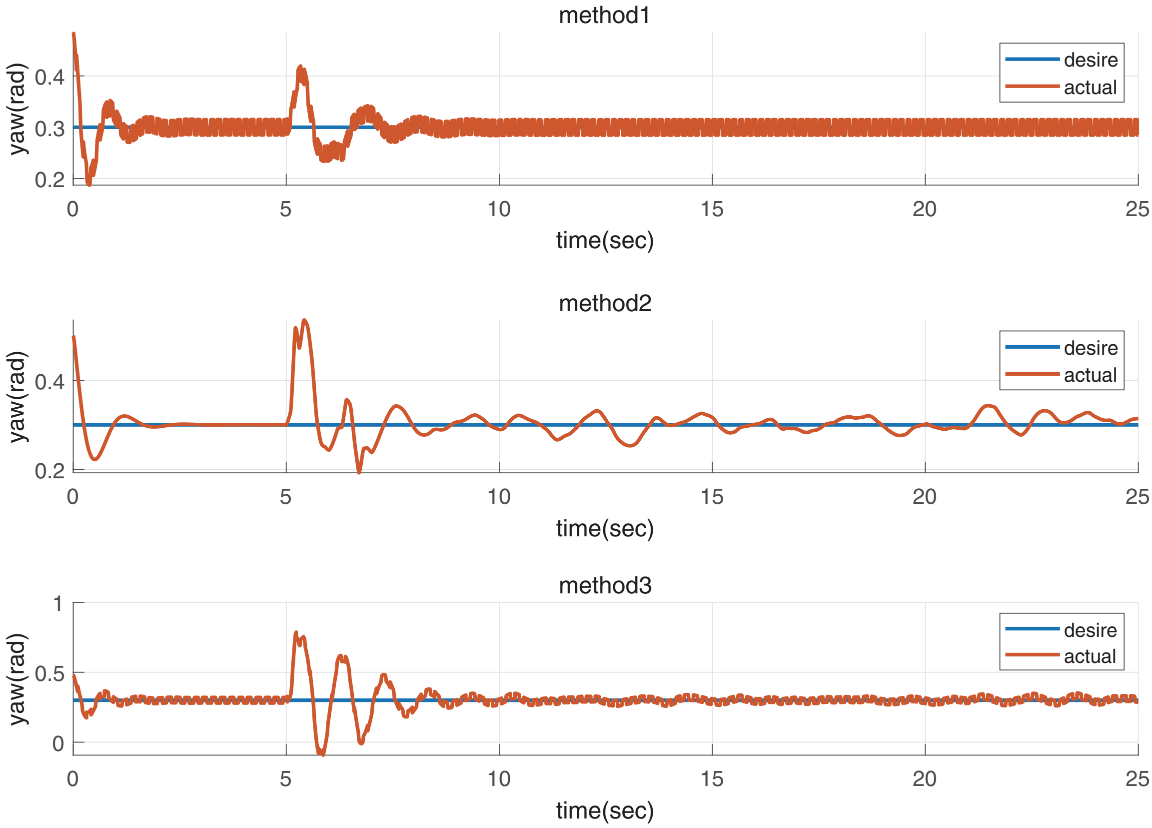

FIGURE 6. Time response of yaw

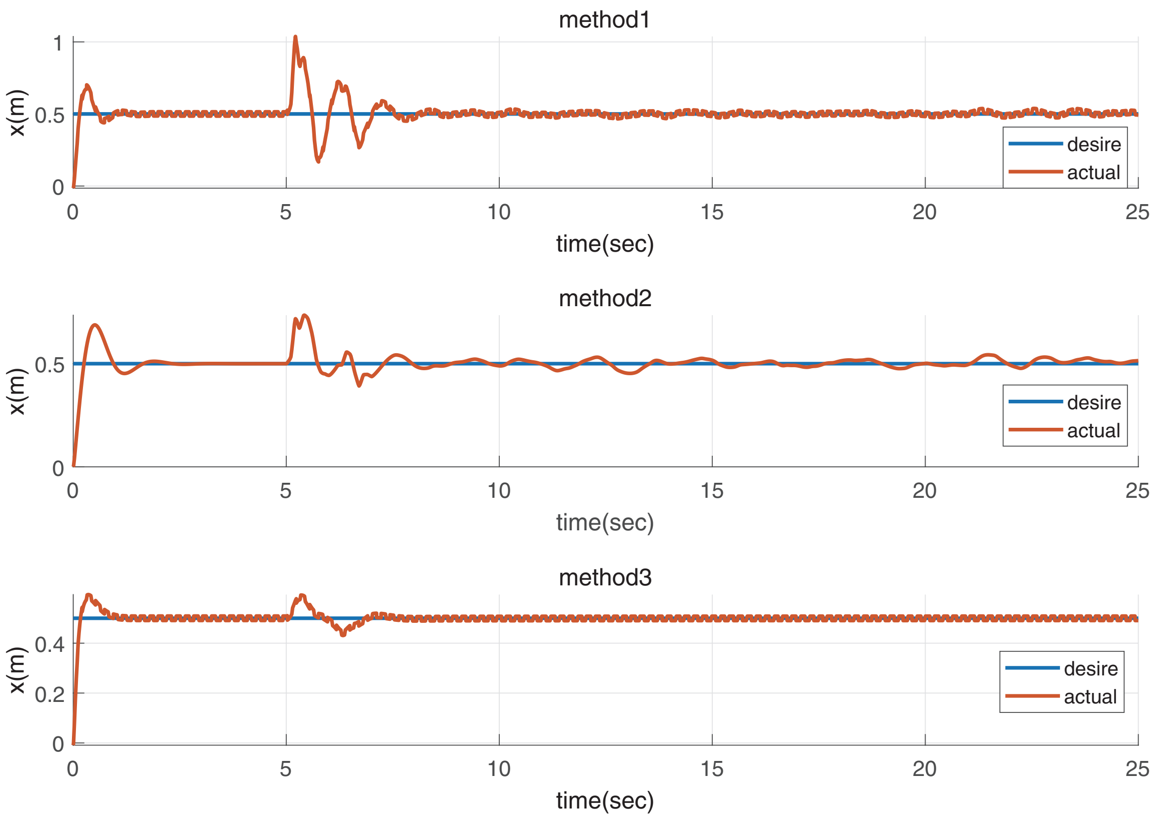

FIGURE 7. Time response of x position

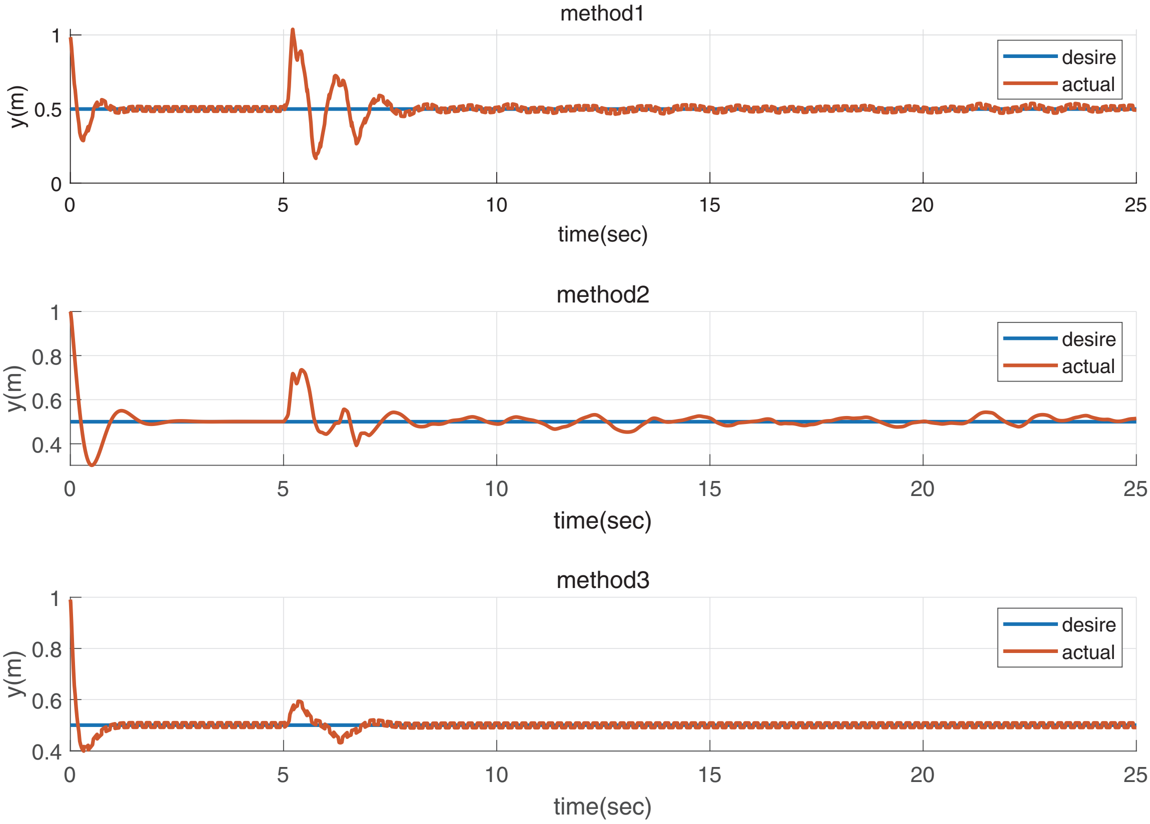

FIGURE 8. Time response of y position

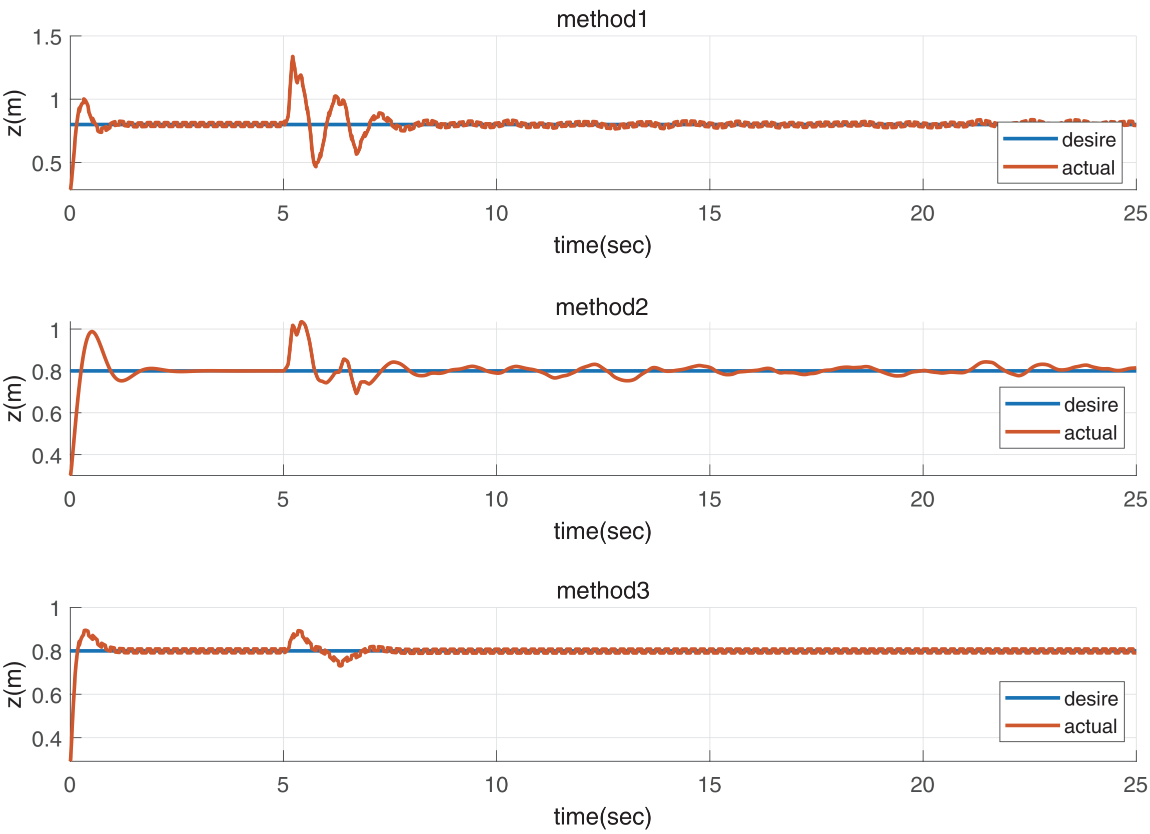

FIGURE 9. Time response of z position

than method 1, and the constraints are never transgressed because of the introduction of BLF. Meanwhile, from Figures 4-9, we can see that method 2 is less sensitive to disturbance. However, as shown in the curves, tracking errors exist in the presence of fault due to the loss of FDD module. Both methods 1 and 2 are not able to meet the mission.

For method 3, Figures 4-6 show that attitude curves converge in about 5 seconds and from Figutrs 7-9 we obtain that the position trajectories can eliminate in about 3 seconds. Simultaneously, the state constraints are never transgressed. To sum up, the conjunction of BLF and NFTSMC makes the tracking trajectory convergent faster and have higher steady precision than methods 1 and 2 without violation of constraints. Furthermore, the control input is also suitable for a quadrotor UAV.

A complete fault-tolerant control system is proposed in this paper, which copes with not only fault detection and isolation but also fault-tolerant control. And the simulation results show strong robustness of the proposed method, which has lots of practical value in engineering application since some practical engineering problems have been considered in this paper. To sum up, the proposed algorithm can deal with constraints well and shows strong robustness to the actuator faults.

5. **Conclusion.** In this subject, a novel FTC method is developed for quadotor with state constraints based on fast nonsingular terminal sliding mode in conjunction with ABLF. The proposed algorithm is a finite-time tracking method with strong robustness. First, an adaptive estimator is presented to detect the accurate unknown actuator fault. Then an FTC law based on NFTDMC is designed to cope with the influence of disturbance and actuator faults. The introduction of ABLF ensures that the sliding mode surface is bounded in a range, and the constraints of the states will never be transgressed. In the simulation, a sliding mode based active fault-tolerant controller and a traditional backstepping algorithm based on ABLF are utilized for contrast and verify the advantages of the proposed method. In future work, more practical flight missions such as time-varying constraints and load will be taken into consideration.

Acknowledgment. This work is supported by the National Science Key Lab Fund project (6142605200402), the National Natural Science Foundation of China (61922042) and the Fundamental Research Funds for the Central Universities (NJ2020004).

REFERENCES

[1] X. Liang, Y. Fang, N. Sun and H. Lin, Nonlinear hierarchical control for unmanned quadrotor transportation systems, *IEEE Trans. Industrial Electronics*, vol.65, no.4, pp.3395-3405, 2018.

[2] M. Vandanipour and M. Khodabandeh, Adaptive fractional order sliding mode control for a quadrotor with a varying load, *Aerospace Science and Technology*, vol.86, pp.737-747, 2019.

[3] M. A. Sayeed and R. Shree, Optimizing unmanned aerial vehicle assisted data collection in cluster based wireless sensor network, *ICIC Express Letters*, vol.13, no.5, pp.367-374, 2019.

[4] B. Wang and Y. Zhang, An adaptive fault-tolerant sliding mode control allocation scheme for multirotor helicopter subject to simultaneous actuator faults, *IEEE Trans. Industrial Electronics*, vol.65, no.5, pp.4227-4236, 2018.

[5] Q. L. Hu, Y. Shi and X. Shao, Adaptive fault-tolerant attitude control for satellite reorientation under input saturation, *Aerospace Science and Technology*, vol.78, pp.171-182, 2018.

[6] Y. M. Zhang, A. Chamseddine, C. A. Rabbath, B. W. Gordon, C.-Y. Su, S. Rakheja, C. Fulford, J. Apkarian and P. Gosselin, Development of advanced FDD and FTC techniques with application to an unmanned quadrotor helicopter testbed, *Journal of the Franklin Institute*, vol.350, no.9, pp.2396-2422, 2013.

[7] F. Chen, R. Jiang, K. Zhang, B. Jiang and G. Tao, Robust backstepping sliding-mode control and observer-based fault estimation for a quadrotor UAV, *IEEE Trans. Industrial Electronics*, vol.63, no.8, pp.5044-5056, 2016.

[8] Z. Song, S. Ling and K. Sun, Adaptive fault tolerant attitude tracking control for miniature rotorcrafts under actuator saturation, *Aerospace Science and Technology*, vol.69, pp.27-38, 2017.
[9] R. C. Avram, X. Zhang and J. Muse, Nonlinear adaptive fault-tolerant quadrotor altitude and attitude tracking with multiple actuator faults, *IEEE Trans. Control Systems Technology*, vol.26, no.2, pp.701-707, 2018.
[10] M. R. Gharib and M. Moavenian, Full dynamics and control of a quadrotor using quantitative feedback theory, *International Journal of Numerical Modelling Electronic Networks, Devices and Fields*, vol.29, no.3, pp.501-519, 2015.
[11] K. D. Young, V. I. Utkin and U. Ozguner, A control engineer's guide to sliding mode control, *IEEE Trans. Control Systems Technology*, vol.7, no.3, pp.328-342, 1999.
[12] H. Alwi and C. Edwards, Fault tolerant control using sliding modes with on-line control allocation, *Automatica*, vol.44, no.7, pp.1859-1866, 2008.
[13] S. Ding, L. Liu and W. X. Zheng, Sliding mode direct yaw-moment control design for in-wheel electric vehicles, *IEEE Trans. Industrial Electronics*, vol.64, no.8, pp.6752-6762, 2017.
[14] Y. Niu and X. Wang, Sliding mode control design for uncertain delay systems with partial actuator degradation, *International Journal of Systems Science*, vol.40, no.4, pp.403-409, 2009.
[15] S. Varma and K. D. Kumar, Fault-tolerant control satellite attitude control using solar radiation pressure based on nonlinear adaptive sliding mode, *Acta Astronautica*, vol.66, nos.3-4, pp.486-500, 2010.
[16] Y. M. Zhang and J. Jiang, Bibliographical review on reconfigurable fault-tolerant control systems, *Annual Reviews in Control*, vol.32, no.2, pp.229-252, 2008.
[17] Z. F. Gao, B. Jiang, P. Shi, M. Qian and J. Lin, Active fault tolerant control design for reusable launch vehicle using adaptive sliding mode technique, *Journal of the Franklin Institute*, vol.349, no.4, pp.1543-1560, 2012.
[18] Z. X. Liu, C. Yuan and Y. M. Zhang, Active fault-tolerant control of unmanned quadrotor helicopter using linear parameter varying technique, *J. Intell. Robot. Syst.*, vol.88, nos.2-4, pp.415-436, 2017.
[19] Y. Ma, B. Jiang and G. Tao, A new multiple-model adaptive actuator failure compensation scheme for a class of nonlinear MIMO systems, *Proc. of the 34th Chinese Control Conference (CCC)*, Hangzhou, pp.6274-6279, 2015.
[20] B. Wang, Y. Shen and Y. Zhang, Active fault-tolerant control for a quadrotor helicopter against actuator faults and model uncertainties, *Aerospace Science and Technology*, vol.99, 2020.
[21] W. Gong, B. Li, Y. Yang, H. Ban and B. Xiao, Fixed-time integral-type sliding mode control for the quadrotor UAV attitude stabilization under actuator failures, *Aerospace Science and Technology*, vol.95, 2019.
[22] D. Q. Mayne, J. B. Rawlings, C. V. Rao and P. O. M. Scokaert, Constrained model predictive control: Stability and optimality, *Automatica*, vol.36, no.6, pp.789-814, 2000.
[23] E. G. Gilbert and I. Kolmanovsky, Fast reference governors for systems with state and control constraints and disturbance inputs, *Robust and Nonlinear Control*, vol.9, no.15, pp.1117-1141, 1999.
[24] T. Hu, Z. Lin and L. Qiu, Stabilization of exponentially unstable linear systems with saturating actuators, *IEEE Trans. Autom. Control*, vol.46, no.9, pp.973-979, 2001.
[25] K. P. Tee, S. S. Ge and E. H. Tay, Barrier Lyapunov functions for the control of output-constrained nonlinear systems, *Automatica*, vol.45, no.4, pp.918-927, 2009.
[26] C. Fu, W. Hong, H. Lu, L. Zhang, X. Guo and Y. Tian, Adaptive robust backstepping attitude control for a multi-rotor unmanned aerial vehicle with time-varying output constraints, *Aerospace Science and Technology*, vol.78, pp.593-603, 2018.
[27] G. V. Raffo, M. G. Ortega and F. R. Rubio, An integral predictive nonlinear H_∞ control structure for a quadrotor helicopter, *Automatica*, vol.46, no.1, pp.29-39, 2010.
[28] Z. Jia, J. Yu, Y. Mei, Y. Chen, Y. Shen and X. Ai, Integral backstepping sliding mode control for quadrotor helicopter under external uncertain disturbances, *Aerospace Science and Technology*, vol.68, pp.299-307, 2017.
[29] K. P. Tee, B. Ren and S. S. Ge, Control of nonlinear systems with time-varying output constraints, *Automatica*, vol.47, no.11, pp.2511-2516, 2011.
[30] B. Jiang and M. Staroswiecki, Actuator fault tolerant control in nonlinear continuous-time systems, *Proc. of the 6th World Congress on Intelligent Control and Automation*, Dalian, pp.5483-5487, 2006.
[31] T. Li, Y. Zhang, B. W. Gordon, Nonlinear fault-tolerant control of a quadrotor UAV based on sliding mode control technique, *IFAC Proceedings Volumes*, vol.45, no.20, pp.1317-1322, 2012.